Cosmic Masers: Proper Motion toward the Next-Generation Large Projects
Proceedings IAU Symposium No. 380, 2024
T. Hirota, H. Imai, K. Menten, & Y. Pihlström, eds.
doi:10.1017/S1743921323001928

Maser science with the next generation Very Large Array (ngVLA)

Todd R. Hunter[1,2]

[1]National Radio Astronomy Observatory, Charlottesville, VA 22903, USA.
email: thunter@nrao.edu

[2]Center for Astrophysics | Harvard & Smithsonian, Cambridge, MA 02138, USA

Abstract. Imaging the bright maser emission produced by the various molecular species from 1.6 to 116 GHz provides a way to probe the kinematics of dense molecular gas at high angular resolution. Unimpeded by the high dust optical depths that affect shorter wavelength (sub)mm observations, the high brightness temperature of these emission lines have become an essential tool for understanding the process of massive star formation. Operating from 1.2–116 GHz, the next generation Very Large Array (ngVLA) of 263 antennas will provide the capabilities needed to fully exploit these powerful tracers, including the ability to resolve accretion and outflow motions down to scales as fine as ∼1-10 au in deeply embedded Galactic star-forming regions, and at sub-pc scales in nearby galaxies. I will summarize the proposed specifications of the ngVLA, describe the current status of the project, and offer examples of future experiments designed to image the vicinity of massive protostars in continuum, thermal lines, and maser lines simultaneously.

Keywords. Radio observatories, Radio interferometers, Astrophysical masers, Interstellar molecules

1. Introduction: The next generation Very Large Array

The 2020 US Decadal Survey of the National Academies (National Academies of Sciences 2021) identified the ngVLA as a high-priority large, PI-driven ground-based facility whose construction should start this decade. With scientific use cases that span imaging, beam forming, and pulsar timing (Murphy *et al.* 2018), the technical baseline of the facility (Selina *et al.* 2018) is summarized in Table 1. A key design choice was to place all antennas in fixed locations, in order to minimize operations costs. The main reflector geometry is an off-axis 18 m-diameter Gregorian with feed low to promote easier maintenance, an rms surface accuracy of 160 μm, and shaped optics to maximize the total system efficiency (>80% in bands 2-5, including digital efficiency). The panels are machined aluminum on a steel backup structure while the feed arm is mostly carbon fiber and the subreflector is composite. The servo performance specification includes a 4° slew and settle in 10 sec. The prototype is under construction in Germany. The current timeline of the project is shown in Table 2, with initial radiometric tests anticipated to begin in late 2024 at 3 cm and 7 mm.

2. Examples of science topics addressed by masers

We list some of the major scientific use cases of maser observations with the ngVLA. These topics are described in more detail in other contributions of this volume.

Table 1. ngVLA technical baseline.

Antennas			Receivers		Correlator / beamformer requirements	
Configuration group	Number	Baseline longest (km)	Band	Frequency (GHz)	Quantity	Requirement (design goal)
Core	114	4.3	1	1.2–3.5	digital efficiency	> 95%
Spiral	54	39	2	3.5–12.3	narrowest channel	< 1 kHz (0.4)
Mid	46	1070	3	12.3–20.5	total channels	>240000
Long	30	8860	4	20.5–34	total bandwidth	> 14 GHz/pol (20)
Total 18m	244	Range (m)	5	30.5–50.5	sub-band width	<250 MHz (218.75)
SBA 6m	19	11–60	6	70–116	# formed beams	10 (50)

Table 2. ngVLA major milestone dates (as of May 2023).

Milestone	Date
Conceptual Design Review (technical)	July 2022
Cost Review	December 2023
Prototype antenna delivery	Late 2024
Preliminary Design Review	Early 2026
Final Design Review (technical)	Mid 2028
Construction	2028-2037
Early Science Operations	Mid 2031
Full Science Operations	Mid 2037

2.1. *Megamaser cosmology*

The use of water megamasers to provide constraints on cosmological parameters is described in Braatz *et al.* (2018). Current precision on H_0 derived from megamaser observations is 3%. Reducing the value to 1% will require at least 50 galaxies measured with $\approx 7\%$ precision. New species of megamasers have been identified recently (Gorski *et al.* 2021).

2.2. *Evolved Stars*

Simultaneous imaging of masers and stellar photosphere with excellent uv coverage is essential to more accurately study the layering of gas properties in evolved stars (Matthews & Claussen 2018). The ability to measure the proper motion of masers over a complete stellar pulsation period will better constrain the pumping mechanism. Multi-band spectra of SiO 2-1 and SiO 1-0, observed contemporaneously in Bands 5 and 6 with ngVLA, will improve the efficiency of surveys of AGB star masers like the BAaDE survey (Sjouwerman *et al.* 2020).

2.3. *Structure of the Milky Way*

Very Long Baseline Interferometry (VLBI) enables parallax and proper motion measurements of masers in massive star-forming regions, which trace the spiral structure of the Milky Way and provide the most accurate estimates of the distance to the Galactic center (Reid *et al.* 2014). The greater sensitivity of ngVLA will provide a more complete view of the Galaxy by enabling routine measurements of these regions on the far side of the Galaxy and greatly expanding the pool of magnetically active young stars for proper motion measurements on the near side (Loinard & Reid 2018).

3. Importance of maser emission in star formation

The process of star formation leads to the concentration of molecular gas to high densities in molecular cloud cores. The potential energy released by gravitational collapse and accretion onto the central protostars heats and excites the surrounding material

https://doi.org/10.1017/S1743921323001928 Published online by Cambridge University Press

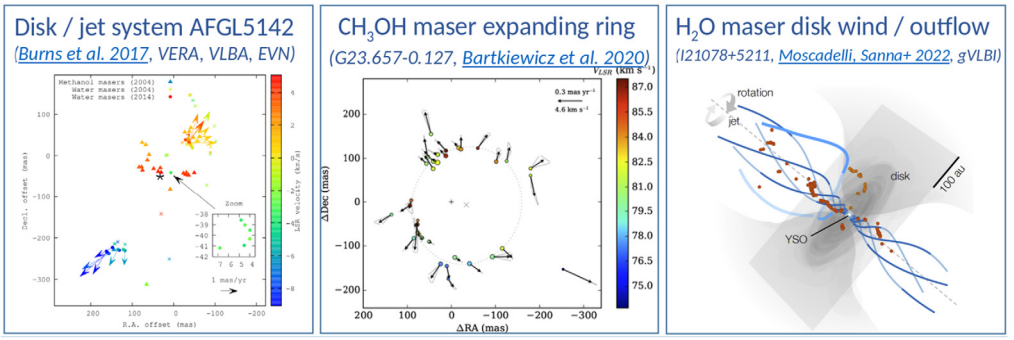

Figure 1. Three examples of kinematic structures traced by VLBI observations of masers around young massive protostars from Burns *et al.* (2017), Bartkiewicz *et al.* (2020), and Moscadelli *et al.* (2022).

through infrared radiation and high velocity bipolar outflows. Both of these feedback mechanisms (radiative and mechanical) naturally produce population inversions between specific pairs of energy levels in several abundant molecules, including H_2O, CH_3OH, OH, NH_3, SiO, and H_2CO. The resulting non-thermal maser emission in the corresponding spectral transitions provides a beacon whose brightness temperature far exceeds the more commonly-excited thermal emission lines. Consequently, maser lines at centimeter wavelengths have traditionally provided a powerful probe of star formation through single-dish surveys and interferometric imaging. In general, they trace hot, dense molecular gas, revealing the kinematics of star-forming material within a few 1000 au from very young stars, including accretion disks and their associated jets, as well as shocks in the outflow lobes where the jets impact ambient gas (Fig. 1).

Masers are generally more prevalent in regions surrounding massive protostars, due to their higher luminosities and more energetic outflows. Furthermore, masers are sensitive indicators of sudden changes in the pumping conditions near the protostars, and, recently, it has been recognized that maser flares, in those lines which are pumped by infrared photons, can be directly associated with bursts of accretion onto the stars. In this context, maser emission provides a unique tool for probing how massive stars form, allowing us to reconstruct the gas dynamics in the vicinity of young stars with tens of Solar masses, as well as to study the accretion process in the time domain.

4. Obscuration of line emission by dust

With the advent of the Atacama Large Millimeter/submillimeter Array (ALMA), imaging thermal lines at high resolution has become easier, and recent results have begun to place previous and ongoing maser studies into better physical context (see, e.g., Orion Source I, Plambeck & Wright 2016; Hirota *et al.* 2017). At the distances of more typical massive star-forming regions, however, the brightness temperature sensitivity of ALMA is still not sufficient to trace the accretion flow and accompanying jet structures that surround massive protostars, because of the high angular and spectral resolution required. Moreover, at the shorter wavelengths of ALMA, the combination of molecular line confusion and high dust opacity toward the hot cores in protoclusters will often block the most interesting details from ALMA's view (van Gelder *et al.* 2022; Nazari *et al.* 2022). In contrast, the centimeter maser transitions propagate unobscured from the innermost regions and provide a strong signal for self-calibration, which enables high dynamic range imaging on long baselines.

https://doi.org/10.1017/S1743921323001928 Published online by Cambridge University Press

5. Importance of angular resolution coupled with sensitivity

Unfortunately, the angular resolution of the VLA is insufficient to resolve the details of accreting gas, particularly in the 6 GHz band where the beamsize is limited to ∼0.3 arcsec. In the handful of nearest examples of massive star formation (d∼1 kpc), this resolution corresponds to 300 au (e.g., Brogan *et al.* 2016). However, in the majority of star-forming sites across the Milky Way at several kpc from the Sun, it exceeds 1000 au, which is often more than the separation of protostars in the centers of massive protoclusters (e.g., Palau *et al.* 2013). Thus, an order of magnitude improvement in angular resolution (requiring at least ∼300 km baselines) is needed to resolve the spatial morphology and kinematics of disks, or other accretion structures, at scales of 10-100 au in a large sample of massive protostars. Such a resolution would also enable three dimensional measurements of gas velocity via multi-epoch proper motions. For instance, with an angular resolution of 10 mas in the bright H_2O maser line, it is possible to determine the maser positions with an accuracy better than 0.1 mas (assuming $S/N > 100$), and then to measure proper motions of order 10 km s^{-1} in a few months only, for sources located up to several kpc distance. Furthermore, proper motion measurements of different maser species toward the same region have the potential to trace simultaneously the complementary kinematic structures around a young star, providing a unique picture of the gas dynamics locally (Sanna *et al.* 2010; Goddi *et al.* 2011). These measurements are currently conducted by means of VLBI observations, but with the small number of available antennas their sensitivity is limited to non-thermal processes exceeding brightness temperatures of $\sim 10^7$ K (e.g. Matsumoto *et al.* 2014; Bartkiewicz *et al.* 2009).

While current VLBI facilities (VLBA, EVN, eMERLIN, KVN, VERA, and LBA) have the requisite angular resolution to trace maser proper motions accurately, studies at these scales currently suffer from poor surface brightness sensitivity, which affects the science in two key ways. First, only the brightest maser spots can be detected, reducing the fidelity with which kinematic structures can be delineated in a single epoch, and reducing the number of potential spots that will persist over multiple epochs (used for proper motion studies). Second, the thermal radio continuum emission which arises in the immediate vicinity of massive protostars, with flux densities of < 1 mJy typically (Cyganowski *et al.* 2011), cannot be observed with the masers simultaneously, leading to (relative) positional uncertainties between the protostellar and maser components. The resulting ambiguity of the dynamical center severely hinders the interpretation of multi-epoch proper motion measurements, which are essential to understand the mass, momentum, and kinetic energy of the inner jet where it transitions into a bipolar molecular outflow. Studying additional objects at scales of 10-100 au in a comprehensive list of maser lines, and with sufficient brightness sensitivity to image simultaneously the associated thermal free-free continuum emission, will be an important task for the ngVLA. These studies will test and expand our current picture of massive star formation into the broader context of the Milky Way.

6. Masers as probes of accretion outbursts

With its proposed frequency span, the ngVLA will uniquely provide access to all of the most important maser transitions from OH at 1.6 GHz to CH_3OH at 109 GHz (Table 3). While each maser transition offers a unique view into any particular region massive star formation, masers can be broadly classified into major categories. The Class II CH_3OH maser lines, primarily at 6.7 GHz, 12.2 GHz, and 19.9 GHz, trace hot molecular gas that is (at least) moderately close to the youngest massive protostars ($\lesssim$ 1000 au), such that they can provide sufficiently intense mid-infrared emission to pump the maser transitions (Sobolev *et al.* 1997; Cragg *et al.* 2005). The light curves of these maser

https://doi.org/10.1017/S1743921323001928 Published online by Cambridge University Press

Table 3. Detected maser lines (>94) in the ngVLA bands; see Table 1 of Menten (2007) for further details. Frequencies in boldface have been detected only during the accretion outburst in G358.93-0.03.

Band	f (GHz)	Species and line frequencies (GHz)	# lines
1	1.2–3.5	ground-state OH (1.612, 1.665, 1.667, 1.720)	4
2	3.5-12.3	excited OH (4.660, 4.750, 4.765, 6.031, 6.035, 6.049)	6
		CH_3OH Class I (9.936)	1
		CH_3OH Class II (6.668, 12.178), (**7**.682, 7.830, Breen *et al.* (2019)), CH_3OH likely Class II: (**12**.229, MacLeod *et al.* (2019))	5
		CH_3OH torsionally-excited: **6**.181, Breen *et al.* (2019)	1
		ortho-H_2CO (4.829)	1
		CH_2NH (5.291) (Gorski *et al.* 2021), CH_3NH_2 (4.364) (Xue *et al.* 2023)	2
3	12.3–20.5	CH_3OH Class II (19.967), **20.346** (MacLeod *et al.* 2019)	2
		$^{13}CH_3OH$: **14.300** (Chen *et al.* 2020)	1
		excited OH (13.441, Baudry *et al.* 1981; Caswell 2004)	1
		NH_3 (**19.757**) (McCarthy *et al.* 2023)	1
4	20.5–34	H_2O (22.235)	1
		CH_3OH J_2-J_1-series Class I (24.9-30.3) Towner *et al.* (e.g., 2017)	15
		CH_3OH Class I (23.445, Voronkov *et al.* 2011)	1
		CH_3OH Class II: 23.121, 28.970 (**27.283, 28.969**, Miao *et al.* (2022))	4
		CH_3OH torsionally-excited: **20.970** (Breen *et al.* 2019), **26.120** (Miao *et al.* 2022)	2
		ortho-NH_3 (3,3) (6,6) (9,9) (12,12) Brogan *et al.* (e.g., 2011)	4
		other NH_3 inversion lines (thermal and/or maser)	>10
		excited OH (23.817, Baudry *et al.* 1981)	1
		HDO: **20.460** (Chen *et al.* 2020)	1
		HNCO: **21.980** (Chen *et al.* 2020)	1
5	30.5–50.5	Class I CH_3OH (36.169, 44.069)	2
		Class II CH_3OH: 37.703, 38.293, 38.452, (**31.977, 34.236, 41.110, 46.558** Miao *et al.* (2022))	3
		SiO 1-0 v=1, rv=2, v=3 (43.122, 42.820, 42.519)	3
		CH_3OH torsionally-excited: **44.955** (Breen *et al.* 2019), **48.708** (Miao *et al.* 2022)	2
		CS 1-0: 48.990 (Ginsburg & Goddi 2019)	1
6	70–116	CH_3OH Class I (84.521, 95.169, 104.300)	3
		CH_3OH Class II (76.247, 76.509, 85.568, 86.615, 104.060, 107.013, 108.894)	7
		CH_3OH torsionally-excited (**99.772, 102.957**, Menten (2019))	2
		HCN J=1-0 vibrationally-excited (89.087)	1
		HCO^+ 1-0: 89.188 (Hakobian & Crutcher 2012)	1
		CS 2-1: 97.980 (Ginsburg & Goddi 2019)	1
		SiO 2-1 v=1, v=2, v=3 (86.243, 85.640, 85.038)	3

species also show intriguing properties. Quasi-periodic flares in one or more Class II CH_3OH maser lines (120–500 days) have been observed in about a dozen objects (e.g., Goedhart *et al.* 2014); in one case, the 4.83 GHz H_2CO maser also shows correlated flaring (Araya *et al.* 2010). Recently, three spectacular accretion outbursts in massive protostars have been accompanied by strong flaring of these lines simultaneously with mid-IR continuum, S255 NIRS3 (Caratti o Garatti *et al.* 2017; Moscadelli *et al.* 2017), NGC 6334 I-MM1 (Hunter *et al.* 2017, 2018; MacLeod *et al.* 2018; Hunter *et al.* 2021), and G358.93-0.03 (Brogan *et al.* 2019; Breen *et al.* 2019; MacLeod *et al.* 2019; Stecklum *et al.* 2021) supporting the idea that maser flares are caused by a variable accretion rate onto the central protostar. The first two of these extraordinary events led to the formation of the international Maser Monitoring Organization (M2O), with the goal of detecting and reporting future maser flares so that interferometers can be alerted to study the accretion event while it is still underway. Such an accretion event is also expected to yield variation in the continuum emission from the thermal jet (Cesaroni *et al.* 2018) and/or the hypercompact HII region (Brogan *et al.* 2018). Since both of these phenomena are

https://doi.org/10.1017/S1743921323001928 Published online by Cambridge University Press

powered by the protostar, the ability of ngVLA to perform simultaneous observations of the continuum and the masers will enable direct measurements of the correlations between them, yielding important constraints on the physics of the accretion mechanism that is currently being explored via hydrodynamic simulations (Elbakyan *et al.* 2023). Furthermore, the fixed antenna layout means that *rapid* follow-up at each necessary angular scale will *always* be possible, no longer limited by the traditional cadence of VLA configurations. This point is especially important since some outbursts rise and fall in just a few weeks (e.g., G36.11+0.55 Yonekura 2022).

The Class II CH_3OH maser lines, along with the 1.6 GHz ground state OH lines and several excited state OH lines which are radiatively pumped (at 4.66 GHz, 4.75 GHz, 4.765 GHz, 6.030 GHz, and 6.035 GHz), are also seen to trace the ionization front of ultracompact HII regions (e.g., Fish & Reid 2007), which are powered by the more evolved massive protostars and Zero-Age Main Sequence (ZAMS) OB stars. Although excited OH lines are generally considered rare, a recent unbiased survey found that the 6.035 GHz line is detected toward nearly 30% of Class II CH_3OH masers and with a similar distribution in Galactic latitude (Avison *et al.* 2016). A similar detection rate is seen in survey of the 4.765 GHz line (Dodson & Ellingsen 2002). A simple explanation is these excited OH masers always occur in the same objects that power Class II masers, but simply have a correspondingly shorter mean lifetime or duty cycle, perhaps reflecting how long they remain above current sensitivity levels following each successive accretion outburst. In rare cases, the main line OH masers can also trace outflow motion (e.g., W75N and W3OH-TW Fish *et al.* 2011; Argon *et al.* 2003).

The strong water maser line at 22 GHz also traces gas close to massive and intermediate mass protostars. Often these lines span a broad (LSR) velocity range, of several tens of km s^{-1}, about the systemic velocity of the young stars, particularly compared to both classes of methanol masers ($\lesssim 10$ km s^{-1}). In some cases, water masers clearly arise from gas in the first few hundred au of the jet, such as in Cepheus A (e.g., Torrelles *et al.* 2011; Chibueze *et al.* 2012), or in bow shocks somewhat further out (e.g., Sanna *et al.* 2012; Burns *et al.* 2016). With continent-scale baselines, proper motion studies of these masers reveal the 3D velocities and orientations of collimated jets and/or wide-angle winds in the inner few 1000 au from the central protostars (e.g., Torrelles *et al.* 2014; Sanna *et al.* 2010). When these studies are combined with high-resolution radio continuum observations of radio thermal jets, they can allow us to quantify the outflow energetics directly produced by the star formation process (e.g., Moscadelli *et al.* 2016; Sanna *et al.* 2016), as opposed to estimates of the molecular outflow energetics that are attainable on scales greater than 0.1 pc (typically through CO isotopologues). Long-term monitoring studies demonstrate that water masers are also highly variable (e.g., Felli *et al.* 2007), and their primary pumping mechanism is not believed to be radiative but collisional. Thus, since water masers are fundamentally produced in specific ranges of gas density and temperature within shocked gas layers, they are likely to trace different types of coherent motions at different stages of protostellar evolution. This is the case, for instance, of the star-forming region W75 N, where the 22 GHz masers (and the radio continuum) show different spatial distributions around two distinct young stars at different evolutionary stages (Carrasco-González *et al.* 2015). The 22 GHz line is also unique in exhibiting the 'superburst' phenomenon, in which brief flares reach 10^5 Jy or more. It has happened in only a few objects including Orion KL (Hirota *et al.* 2014, and references therein) and G25.65+1.05 (Lekht *et al.* 2018), but it has repeated in both, and appears to be due to interaction of the jet with high density clumps in the ambient gas, but within a few thousand au of the central protostar. In addition to Galactic studies, the detection and imaging of water masers in nearby star-forming galaxies provides a powerful probe of optically-obscured areas of star formation like the overlap region of the Antennae (Brogan *et al.* 2010).

https://doi.org/10.1017/S1743921323001928 Published online by Cambridge University Press

Maser emission from the vibrationally-excited levels of SiO offers a powerful (though rare) probe of the innermost hot gas surrounding massive protostars. For example, in one spectacular nearby case (Orion KL), movies of the vibrationally-excited SiO J=1-0, v=0 and v=1 transitions at 43 GHz have revealed a complicated structure of disk rotation and outflow (Matthews *et al.* 2010). Additional massive protostars (at greater distances) have recently been detected in these lines (Cordiner *et al.* 2016; Ginsburg *et al.* 2015; Zapata *et al.* 2009). The increased sensitivity of the ngVLA will no doubt yield further detections and enable new detailed images of the inner accretion structures in these objects.

7. Connection to thermal lines

Even with the sensitivity of ngVLA, masers will provide only a partial view of circumprotostellar material. We will still rely on thermal lines to complete the picture and provide quantitative measurements of gas temperature and column density. The lines traditionally used at the VLA like NH_3, and 3 mm lines like CH_3CN 6-5 at 110 GHz will be exploited to higher angular resolution than currently possible. In addition, HDO $1_{1,0}$–$1_{1,1}$ at 80.578 GHz will provide a powerful tracer of the thermal water reservoir. Not yet observed by ALMA (it lies in the range of the Band 2 receiver, which is still in the construction phase), this transition traces the hot corino IRAS 16293-2422 B (Parise *et al.* 2005). As shown by the energy level diagram (Kulczak-Jastrzebska 2016), the E_{lower} of this transition is 47 K and its lower state is the upper state of the 893.636 GHz transition to the ground state $0_{0,0}$ in ALMA Band 10, which was recently observed by McGuire *et al.* (2018) in NGC 6334 I. This line beautifully traces a thermal gas outflow from the outbursting protostar MM1, strikingly aligned and interspersed with a linear distribution of 22 GHz maser spots, and demonstrates the potential of the 80.578 GHz line to probe similar structures. Finally, variations in the intensities of thermal lines in response to accretion outbursts is a promising line of research with initial results in the periodic CH_3OH maser G24.33+0.14 (Hirota *et al.* 2022).

8. Conclusion

In summary, with the ability to image the non-thermal and thermal processes simultaneously, it will finally be possible to link the studies of the 3D gas dynamics (using the masers) with studies of the physical conditions of the ionized and molecular gas (using the continuum and strong, compact thermal lines like ammonia, respectively) at the same spatial resolution. Also, the ability to acquire high-fidelity images of all of these maser lines in just a few tunings will promote more uniform surveys of massive protostars as well as enable rapid monitoring of protostars currently undergoing an accretion outburst. Furthermore, the broader bandwidth receivers will provide more robust measurements of the spectral index of the continuum emission by promoting the ability to obtain all the necessary observations at a common epoch. With the improved continuum sensitivity, young lower-mass T Tauri stars, which are chromospherically active stars associated with highly-variable faint (synchrotron) radio continuum emission, will be also detected in the lower frequency bands (e.g., Band 2, Forbrich *et al.* 2017), providing information about the low-mass population of protoclusters. Finally, the high spectral resolution and full polarization capability of the ngVLA will allow measurements of the magnetic field in the masing molecular gas via the Zeeman effect in methanol and water, which is a fundamental quantity for understanding the physics of star formation.

https://doi.org/10.1017/S1743921323001928 Published online by Cambridge University Press

Acknowledgements

The National Radio Astronomy Observatory is a facility of the National Science Foundation operated under agreement by Associated Universities, Inc. This research used the https://www.splatalogue.net spectroscopy database (Remijan *et al.* 2016).

References

Araya, E. *et al.* 2010, *ApJ*, 717, 133
Argon, A. L., Reid, M. J., & Menten, K. M. 2003, *ApJ*, 593, 925
Avison, A., Quinn, L. J., Fuller, G. A., *et al.* 2016, *MNRAS*, 461, 136
Bartkiewicz, A., Sanna, A., Szymczak, M., *et al.* 2020, *A&A*, 637, A15
Bartkiewicz, A., Szymczak, M., van Langevelde, H. J., Richards, A. M. S., & Pihlström, Y. M. 2009, *A&A*, 502, 155
Baudry, A., Walmsley, C. M., Winnberg, A., & Wilson, T. L. 1981, *A&A*, 102, 287
Braatz, J., Pesce, D., Condon, J., *et al.* 2018, *Science with a Next Generation Very Large Array*, 517, 821
Breen, S. L., Sobolev, A. M., Kaczmarek, J. F., *et al.* 2019, *ApJL*, 876, L25
Brogan, C. L., Hunter, T. R., Towner, A. P. M., *et al.* 2019, *ApJL*, 881, L39
Brogan, C.L., *et al.* 2018, in *Proc. of IAU Symp.* 336, ed. A. Tarchi, M.J. Reid & P. Castangia, Cambridge University Press
Brogan, C.L., *et al.* 2016, *ApJ*, 832, 187
Brogan, C. L., Hunter, T. R., Cyganowski, C. J., *et al.* 2011, *ApJL*, 739, L16
Brogan, C., Johnson, K., & Darling, J. 2010, *ApJL*, 716, L51
Burns, R. A., Handa, T., Imai, H., *et al.* 2017, *MNRAS*, 467, 2367
Burns, R. A., Handa, T., Nagayama, T., Sunada, K., & Omodaka, T. 2016, *MNRAS*, 460, 283
Caratti o Garatti, A., Stecklum, B., Garcia Lopez, R., *et al.* 2017, *Nature Physics*, 13, 276
Carrasco-González, C., Torrelles, J. M., Cantó, J., *et al.* 2015, *Science*, 348, 114
Caswell, J. L. 2004, *MNRAS*, 352, 101
Cesaroni, R., Moscadelli, L., Neri, R., *et al.* 2018, *A&A*, 612, 103
Chen, X., Sobolev, A. M., Ren, Z.-Y., *et al.* 2020, *Nature Astronomy*, 4, 1170.
Chibueze, J. O., Imai, H., Tafoya, D., *et al.* 2012, *ApJ*, 748, 146
Cordiner, M. A., Boogert, A. C. A., Charnley, S. B., *et al.* 2016, *ApJ*, 828, 51
Cragg, D. M., Sobolev, A. M., & Godfrey, P. D. 2005, *MNRAS*, 360, 533
Cyganowski, C. J., Brogan, C. L., Hunter, T. R., & Churchwell, E. 2011, *ApJ*, 743, 56
Dodson, R. G., & Ellingsen, S. P. 2002, *MNRAS*, 333, 307
Elbakyan, V. G., Nayakshin, S., Meyer, D. M.-A., *et al.* 2023, *MNRAS*, 518, 791
Felli, M., Brand, J., Cesaroni, R., *et al.* 2007, *A&A*, 476, 373
Fish, V. L., Gray, M., Goss, W. M., & Richards, A. M. S. 2011, *MNRAS*, 417, 555
Fish, V. L., & Reid, M. J. 2007, *ApJ*, 670, 1159
Forbrich, J., Reid, M. J., Menten, K. M., *et al.* 2017, *ApJ*, 844, 109
Ginsburg, A. & Goddi, C. 2019, *AJ*, 158, 208.
Ginsburg, A., Walsh, A., Henkel, C., *et al.* 2015, *A&A*, 584, L7
Goddi, C., Moscadelli, L., & Sanna, A. 2011, *A&A*, 535, L8
Goedhart, S., *et al.* 2014, *MNRAS*, 437, 1808
Gorski, M. D., Aalto, S., Mangum, J., *et al.* 2021, *A&A*, 654, A110.
Hakobian, N. S. & Crutcher, R. M. 2012, *ApJL*, 758, L18.
Hirota, T., Wolak, P., Hunter, T. R., *et al.* 2022, *PASJ*, 74, 1234
Hirota, T., Machida, M. N., Matsushita, Y., *et al.* 2017, *Nature Astronomy*, 1, 0146
Hirota, T., Tsuboi, M., Kurono, Y., *et al.* 2014, *PASJ*, 66, 106
Hunter, T. R., Brogan, C. L., De Buizer, J. M., *et al.* 2021, *ApJL*, 912, L17
Hunter, T. R., Brogan, C. L., *et al.* 2018, *ApJ*, 854, 170
Hunter, T. R., Brogan, C. L., MacLeod, G. C., *et al.* 2017, *ApJL*, 837, L29
Kulczak-Jastrzebska, M. 2016, *Acta Astronomica*, 66, 239
Lekht, E. E., *et al.* 2018, *Astronomy Reports*, 62, 213

Loinard, L. & Reid, M. J. 2018, Science with a Next Generation Very Large Array, 517, 411
MacLeod, G. C., Sugiyama, K., Hunter, T. R., *et al.* 2019, *MNRAS*, 489, 3981
MacLeod, G. C., *et al.* 2018, *MNRAS*, 478, 1077
Matsumoto, N., Hirota, T., Sugiyama, K., *et al.* 2014, *ApJL*, 789, L1
Matthews, L. D. & Claussen, M. J. 2018, *Science with a Next Generation Very Large Array*, 517, 281
Matthews, L., *et al.* 2010, *ApJ*, 708, 80
McCarthy, T. P., Breen, S. L., Kaczmarek, J. F., *et al.* 2023, *MNRAS*, 522, 4728.
McGuire, B. A., Brogan, C. L., Hunter, T. R., *et al.* 2018, *ApJL*, 863, L35
Menten, K.M. 2019, private communication
Menten, K. M. 2007, *Astrophysical Masers and their Environments*, IAU Symposium 242, 496
Miao, D., Chen, X., Song, S.-M., *et al.* 2022, *ApJS*, 263, 9
Moscadelli, L., Sanna, A., Beuther, H., *et al.* 2022, *Nature Astronomy*, 6, 1068
Moscadelli, L., Sanna, A., Goddi, C., *et al.* 2017, *A&A*, 600, L8
Moscadelli, L., Sánchez-Monge, Á., Goddi, C., *et al.* 2016, *A&A*, 585, A71
Murphy, E. J., Bolatto, A., Chatterjee, S., *et al.* 2018, *Science with a Next Generation VLA*, 517, 3
National Academies of Sciences, E. 2021, *Pathways to Discovery in Astronomy and Astrophysics for the 2020s*, Washington, DC: The National Academies Press, 2021
Nazari, P., Tabone, B., Rosotti, G. P., *et al.* 2022, *A&A*, 663, A58
Palau, A., Fuente, A., Girart, J. M., *et al.* 2013, *ApJ*, 762, 120
Parise, B., Caux, E., Castets, A., *et al.* 2005, *A&A*, 431, 547
Plambeck, R. L., & Wright, M. C. H. 2016, *ApJ*, 833, 219
Reid, M. J., Menten, K. M., Brunthaler, A., *et al.* 2014, *ApJ*, 783, 130
Remijan, A., Seifert, N. A., & McGuire, B. A. 2016, *71st Intl. Symp. on Molecular Spectroscopy*, FB11
Sanna, A., Moscadelli, L., Cesaroni, R., *et al.* 2016, *A&A*, 596, L2
Sanna, A., Reid, M. J., Carrasco-González, C., *et al.* 2012, *ApJ*, 745, 191
Sanna, A., Moscadelli, L., Cesaroni, R., *et al.* 2010, *A&A*, 517, A78
Selina, R. J., Murphy, E. J., McKinnon, M., *et al.* 2018, *Science with a Next Generation VLA*, 517, 15
Sjouwerman, L. O., Pihlström, Y. M., *et al.* 2020, *Galactic Dynamics in the Era of Large Surveys*, 353, 45
Sobolev, A. M., Cragg, D. M., & Godfrey, P. D. 1997, *A&A*, 324, 211
Stecklum, B., Wolf, V., Linz, H., *et al.* 2021, *A&A*, 646, A161
Torrelles, J. M., Trinidad, M. A., Curiel, S., *et al.* 2014, *MNRAS*, 437, 3803
Torrelles, J. M., Patel, N. A., Curiel, S., *et al.* 2011, *MNRAS*, 410, 627
Towner, A. P. M., Brogan, C. L., Hunter, T. R., *et al.* 2017, *ApJS*, 230, 22
Voronkov, M. A., Walsh, A. J., Caswell, J. L., *et al.* 2011, *MNRAS*, 413, 2339
Xue, C., *et al.* 2023, in preparation
van Gelder, M. L., Nazari, P., Tabone, B., *et al.* 2022, *A&A*, 662, A67
Yonekura, Y., 2022, private communication
Zapata, L. A., Menten, K., Reid, M., & Beuther, H. 2009, *ApJ*, 691, 332

https://doi.org/10.1017/S1743921323001928 Published online by Cambridge University Press